

# Double quartz tuning fork sensor for low temperature atomic force and scanning tunneling microscopy

M. Heyde,<sup>a)</sup> M. Kulawik, H.-P. Rust, and H.-J. Freund

*Fritz-Haber-Institut der Max-Planck-Gesellschaft, Faradayweg 4-6, D-14195 Berlin, Germany*

(Received 30 September 2003; accepted 5 April 2004; published online 29 June 2004)

A double quartz tuning fork sensor for low temperature ultrahigh vacuum atomic force and scanning tunneling microscopy is presented. The features of the new sensor are discussed and compared to a single asymmetric tuning fork assembly. In addition, a low temperature ac signal amplifier has been developed to pick up the oscillation amplitude of the tuning fork. Current consumption and amplification factor versus the supply voltage of the amplifier as well as the magnitude response of the sensor have been measured at room temperature, 77 and 4 K. Atomically resolved images of a Ag(111) surface and single Ag atoms on Ag(111) were recorded in the scanning tunneling microscopy mode. Initial atomic force measurements are shown that reveal step resolution on a NiAl(110) surface. © 2004 American Institute of Physics. [DOI: 10.1063/1.1765753]

## I. INTRODUCTION

Atomic force microscopy (AFM) and scanning tunneling microscopy (STM) are the most important tools for the investigation of surfaces on the atomic scale in real space. While STM is sensitive to the local density of states and requires a conductive surface, AFM can also be used on insulating samples. Essential for achieving atomic resolution with an AFM is a force detector with low noise performance and enhanced sensitivity to short-range forces. For detailed analysis and interpretation of surface structures, an image sensor with the capability to record AFM and STM images on the same surface area is highly desirable. Compared to many low temperature (LT) ultrahigh vacuum (UHV) STM experiments that demonstrate atomic resolution the number of such results obtained by LT UHV AFM is still small.<sup>1</sup> An important reason why is that a typical AFM requires a sensor to measure deflection of the cantilever that operates at LT and that the relative position of the cantilever and the deflection sensor has to be adjustable or remain within the operating range of the deflection sensor at all temperatures. LT UHV AFM instrumentation based on tunneling,<sup>2</sup> fiber-optic interferometry,<sup>3,4</sup> and laser beam deflection devices<sup>5,6</sup> has been described. Self-sensing devices such as piezoresistive<sup>7,8</sup> and piezoelectric cantilevers<sup>9-11</sup> have also been presented which allow one to simplify the design of a force sensor. Early developments in force detection techniques, in particular, the introduction of the frequency modulation technique<sup>12</sup> in dynamic AFM,<sup>13</sup> have made it possible to achieve true atomic resolution. Atomically resolved dynamic AFM images of silicon (111)-(7×7) surface reconstruction have been presented using laser beam deflection techniques<sup>6</sup> as well as piezoresistive cantilevers<sup>7</sup> and piezoelectric quartz tuning forks.<sup>14</sup> Piezoelectric quartz tuning forks were originally introduced into scanning probe microscopy for use in scanning near field acoustic microscopy<sup>15</sup> and later as dis-

tance control for scanning near field optical microscopes.<sup>16</sup> Several other implementations of tuning forks have been reported.<sup>17,18</sup> Here we present the design of a double tuning fork sensor that works at low temperatures.

## II. PROPERTIES OF A SINGLE ASYMMETRIC TUNING FORK SENSOR

Quartz tuning forks for watches are masterpieces of ingenuity. They are small and robust because of their symmetrical design, and extremely stable in frequency. When used as a frequency normal in watches, the tuning fork is supported at vibrational nodes by electrical contacts and fork prongs swing against each other. As a dynamic AFM sensor as used by Giessibl,<sup>10</sup> one prong is glued at a carrier and a tip is mounted to one electrode of the other prong. The symmetry of this assembly is broken and the tuning fork can now be thought of as a beam fixed at one end. Such a system has several eigenmodes, the first nine of which have been calculated [Figs. 1(a)–1(i)].<sup>19</sup> Mode two is mechanically excited by a piezo actuator. If the system were ideal, no coupling to the other modes occurs and the prong oscillates only in mode two [Fig. 1(b)]. But in practice, especially if a tip is mounted at the prong, the system is not ideal and coupling between eigenmodes will occur. The appearance of twofold image features due to lateral tip oscillation has been reported.<sup>20</sup> For atomic resolution images coupling between the 2nd mode (excited mode) and the 1st and 5th modes (parallel and torsion modes) could cause double images with a distance of the order of an angstrom apart because the tip moves parallel and vertical to the surface and the end atom of the tip describes a Lissajou figure. Torsion mode five especially could be excited if the center of gravity of the tip-fork assembly is not on the axis of symmetry. As a result of the mechanical dimensions, the lowest frequency is the oscillation parallel to the sample surface [Fig. 1(a)]. This eigenmode is also excited by a nonideal assembly. Lateral movement of the tip can be minimized by a symmetrically fixed tip, but it cannot be avoided completely for a single tuning fork sensor.

<sup>a)</sup>Electronic mail: heyde@fhi-berlin.mpg.de

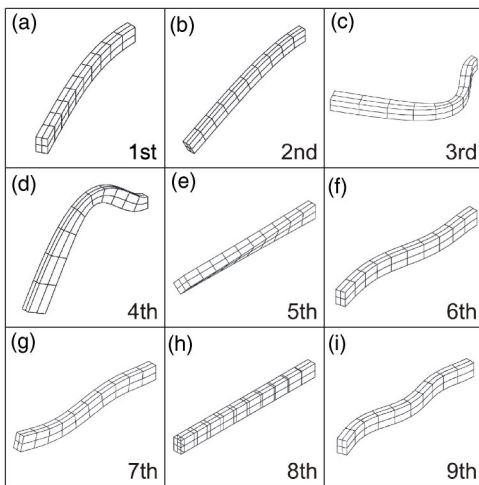


FIG. 1. First nine calculated eigenmodes of a beam fixed at one end (Ref. 19).

### III. DOUBLE TUNING FORK SENSOR

In order to reduce the lateral and torsion eigenmodes we have developed a special double tuning fork design (Fig. 2). The two tuning forks are combined in a V-shaped arrangement. Coupling can only occur via mode eight [Fig. 1(h)], which has a higher resonance frequency and lower amplitude compared to mode two, and is therefore minimal. This design has other advantages: The mass of the tip does not lower the resonance frequency as much as in the single tuning fork case due to the higher force constant of the two combined tuning forks (TF1, TF2). Furthermore, we have an additional electrical sensor available. The second tuning fork (TF2) allows us to measure vibrational information without any tunneling contribution. The high stiffness and the design of the sensor offer the possibility of obtaining AFM and STM images either at the same time (by averaging the tunneling current during acquisition, again taking advantage of the small oscillation amplitudes) or sequentially, but at the same location (by switching off the oscillation; the high stiffness then prevents a jump to contact and reduces noise due to cantilever vibrations). The steps used to build a double tuning fork sensor are described in the following. First, the commercially available quartz tuning forks<sup>21</sup> are removed from their her-

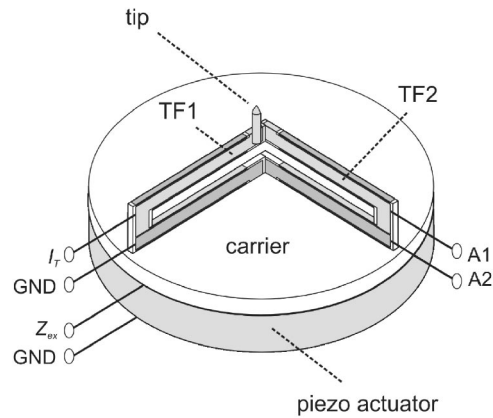


FIG. 2. Schematic of the double tuning fork assembly.

metically sealed canisters. The tuning forks used in the experiments have a bare resonance frequency of  $f_0 = 32\,768\text{ Hz}$  ( $= 2^{15}\text{ Hz}$ ), width  $w = 0.3\text{ mm}$ , length of one prong  $l = 3.5\text{ mm}$  and thickness  $t = 0.6\text{ mm}$ . With the Young's modulus of quartz  $E = 7.87 \times 10^{10}\text{ N/m}^2$  the theoretical force constant of a beam fixed at one end of the single tuning fork used was calculated to be  $k = \frac{1}{4}Ew(t/l)^3 = 30\,000\text{ N/m}$ .<sup>22</sup> One prong of the tuning fork (TF1) is affixed with Torr Seal<sup>23</sup> to a Macor plate, which is mounted to the  $z$  piezo of the microscope head. The Torr Seal is cured at  $100\text{ }^\circ\text{C}$  for 1 h. Afterward, the second tuning fork (TF2) is attached to the Macor carrier, mounted such that the free prongs are glued together as shown in Fig. 2. The Macor carrier is fitted with wires to make electrical connection to the four electrodes of the double tuning fork assembly. A tip made of W or Pt/Ir wire with a typical diameter of  $0.25\text{ }\mu\text{m}$  is glued to one of the tuning fork arms and is electrically connected to one of the four electrodes of the tuning fork assembly by silver epoxy. A tungsten tip can be electrochemically etched by the double lamella drop-off etching procedure.<sup>24</sup>

The tip prepared on the double tuning fork sensor may be used as a tunneling tip (STM mode) or as a force sensor (dynamic AFM mode) without any modification to the microscope system. This gives simultaneous access to two complementary imaging modes at various temperatures with-

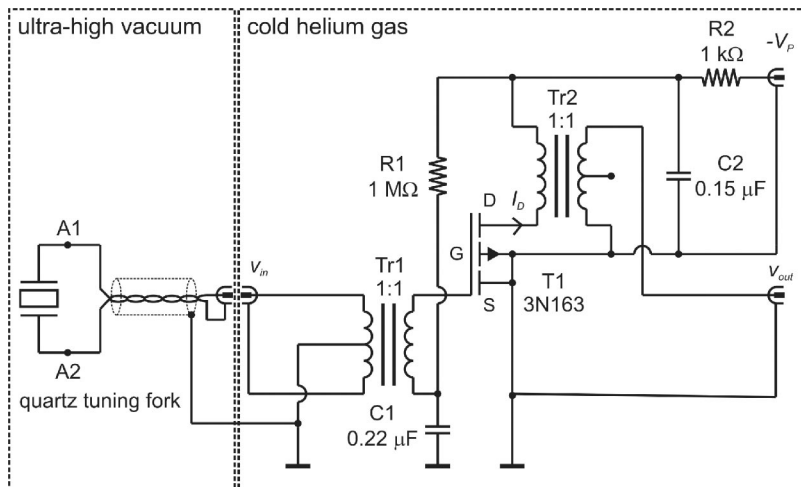


FIG. 3. Circuit diagram of the low temperature pre-amplifier for readout of the electrical tuning fork oscillation amplitude (TF2).

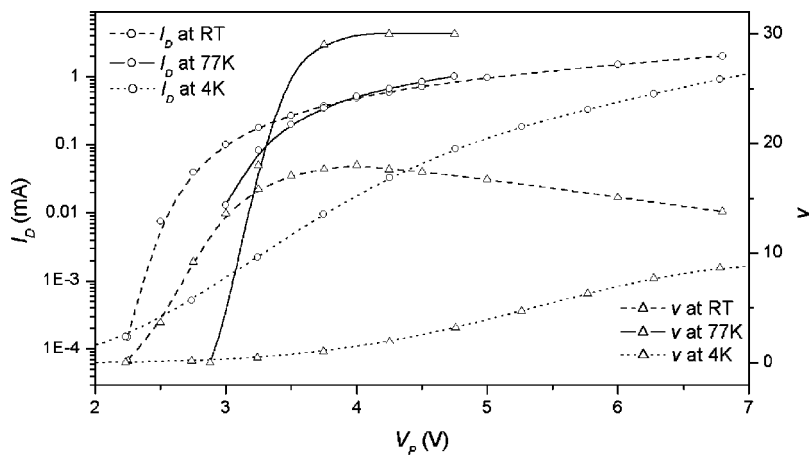


FIG. 4. Supply current and amplification vs the power supply voltage at RT, 77 and 4 K. The amplification  $v$  is defined by  $v = v_{out}/v_{in}$ .

out the need of tip exchange. To convert mechanical oscillation of the tuning forks into an electrical signal, a low temperature ac amplifier has been developed. The need for such an amplifier is to keep the length of the signal lines between the quartz tuning fork and the amplifier input as short as possible to reduce coupled-in background noise and stray capacitance. So it is necessary for the amplifier to work in a temperature range between room temperature and 4 K, the temperature of liquid helium. The amplifier is located directly on top of the microscope flange, outside the ultrahigh vacuum (for details see Sec. IV). An electrical signal equivalent to the mechanical oscillation amplitude is picked up from tuning fork TF2 (contacts A1 and A2, Fig. 2) and fed into the amplifier via shielded twisted pair wires symmetrically to ground it to the audio transformer<sup>25</sup> Tr1 [Fig. 3(a)]. A slightly different setup with an asymmetric readout of the tuning fork oscillation amplitude achieved by exchanging audio transformer Tr1 with a 1 nF capacitor and a 10 M $\Omega$  resistor for biasing has been successfully tested also. The signal is then coupled to the gate of a  $p$ -channel enhancement-mode metal-oxide-semiconductor (MOS) transistor (T1).<sup>26</sup> For such transistors charge carriers are injected from the source and are essentially independent of the temperature, allowing operating temperatures down to 4 K. Also the very low gate leakage current and the relatively low frequency range of the tuning fork assembly between 15 and 30 kHz make this transistor superior to gallium arsenide metal-semiconductor field effect transistors (MESFETs) for this application.

The amplified signal is coupled via transformer<sup>25</sup> Tr2 to the output. Low pass  $RC$  filters ( $R1C1, R2C2$ ) reduce the noise level at the voltage supply line. Metal film resistors are used, because carbon resistors increase their value 100–1000 times when cooled down to liquid helium temperature compared to that at room temperature. In this circuit, the drain-source and the gate-source voltage have the same value and are driven by the power supply voltage  $V_p$ , which has to be adjusted according to the operating temperature (Fig. 4).  $V_p$  is tuned to a value where the supply current, and therefore power dissipation of the amplifier, is as low as possible for a desired amplification factor  $v$ . Power dissipation is a crucial point, because a few milliwatts can increase the temperature of the microscope by one or two degrees kelvin. Typical

magnitude response curves of the double tuning fork assembly are shown in Fig. 5. Phase and amplitude versus the driving frequency are shown at room temperature (RT), 77 and 4 K, in ultrahigh vacuum. The resonance frequency is  $f_0 = 16\,529$  Hz at RT,  $f_0 = 16\,641$  Hz at 77 K, and  $f_0 = 16\,649$  Hz at 4 K and the quality factor is  $Q = 575$  at RT,  $Q = 8500$  at 77 K, and  $Q = 16\,000$  at 4 K.  $Q$  is given by the ratio of the resonance frequency  $f_0$  and the full bandwidth at 0.707 of the maximum amplitude,  $Q = f_0/\Delta f$ .<sup>27</sup>

The double tuning fork assembly is operated by the sensor controller/FM-detector easyPLL from Nanosurf.<sup>28</sup> The sensor is mechanically excited by a dither piezo (Fig. 2), which is part of the  $z$  piezo and driven by the easyPLL's voltage controlled frequency generator. To scale down the excitation voltage from the easyPLL, a 1000:1 voltage divider, residing close to the microscope head, is used. The generator's frequency is set by the easyPLL FM detector such that the sensor's oscillation has a 90° shift in phase with respect to the excitation frequency. This ensures that the sensor is always excited at its resonance frequency. If the resonance frequency of the sensor is altered by interaction of the probe with the sample, the frequency of the generator is automatically tracked to achieve the 90° phase shift and to correct the resonance frequency. The sensor amplitude was calibrated by measuring the  $z$  piezo displacement and the

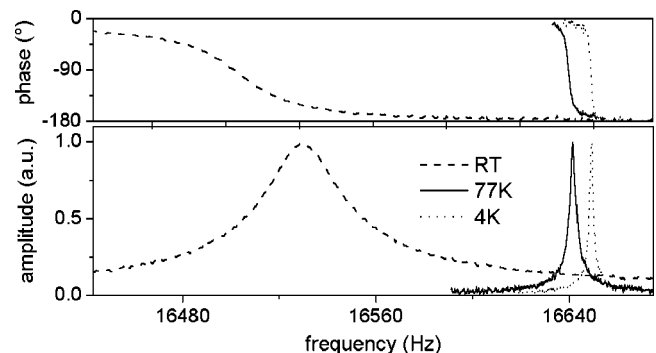


FIG. 5. Typical magnitude response curves of the double tuning fork assembly at RT, 77 and 4 K, in ultrahigh vacuum. Phase and amplitude vs the driving frequency. The signal to noise (S/N) voltage ratio for a bandwidth of 0.5 Hz was measured to be S/N = 60 dB. The sensitivity is 0.5  $\mu$ V/pm based on the input voltage of the low temperature amplifier (see Fig. 3).

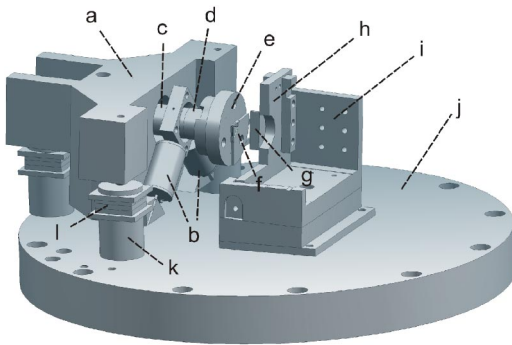


FIG. 6. Schematic of the microscope and the support stage: (a) Walker unit, (b)  $x,y$  piezo and (c)  $z$  piezo of the tripod scanner unit, (d)  $z$  excitation piezo, (e) sensor carrier, (f) tuning fork assembly, (g) sample, (h) sample holder, (i) sample support, (j) support stage, (k) walker support, and (l) shear stack piezos. The support stage has a diameter of 100 mm.

sensor voltage as a function of the exciting voltage of the dither piezo in constant current STM mode.

#### IV. INITIAL EXPERIMENTAL RESULTS

The LT microscope system is based on the design of a helium cooled STM originally invented by Eigler and co-workers.<sup>29</sup> The LT UHV AFM and STM will be briefly discussed.<sup>30,31</sup> The UHV system is equipped with sample storage and utilities for *in situ* sample preparation including a sputter gun, an evaporator, and a residual gas analyzer. The entire system is mounted on a frame carried by active vibration isolation legs purchased from Halcyonics<sup>32</sup> which in turn rest on a separate foundation to decouple it from building vibration. The microscope has been designed to support the piezoelectric quartz tuning fork assembly as a force and tunneling sensor. A schematic of the microscope head is given in Fig. 6. The microscope head allows coarse tip-sample approach and lateral positioning using stick-slip motion. The scanning unit is a tripod assembly made up of three tube piezos. With a maximum driving voltage of  $\pm 125$  V it gives a lateral scan range of 640 nm and a  $z$  range of 928 nm at room temperature. At 77 K the lateral range is 340 nm and the  $z$  range is 490 nm and at 4 K the lateral range is 225 nm and the  $z$  range is 325 nm. A control unit by Nanotech Electronics<sup>33</sup> is used for scan control and data acquisition. Feedback can be switched from STM to AFM mode. Figure 7 demonstrates the performance of the double tuning fork

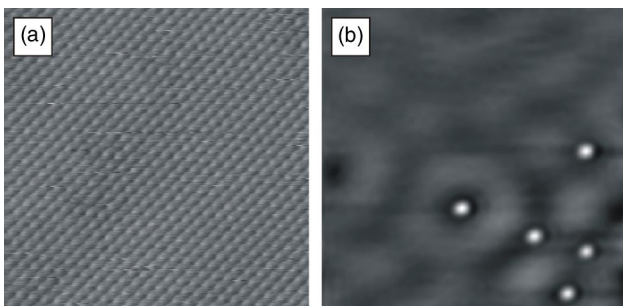


FIG. 7. (a) Atomically resolved STM image on Ag(111), taken at 4 K with  $V_S=20$  mV,  $I_T=5$  pA, and  $7\text{ nm}\times 7\text{ nm}$ . (b) Single silver atoms on a Ag(111) with surface state waves,  $T=4$  K,  $V_S=5$  mV,  $I_T=0.1$  nA, and  $17.7\text{ nm}\times 17.7\text{ nm}$ .

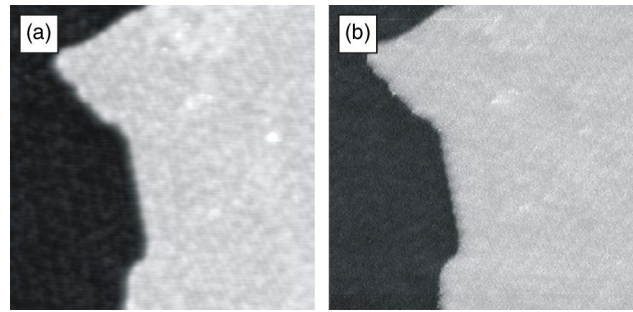


FIG. 8. (a) Thin  $\text{Al}_2\text{O}_3$  film on NiAl(110) imaged at 4 K in STM mode,  $V_S=-1000$  mV,  $I_T=300$  pA,  $40\text{ nm}\times 40\text{ nm}$ . (b) Same area in dynamic AFM mode,  $V_S=-1000$  mV,  $\Delta f=-50.0$  Hz,  $A=0.1$  nm, and  $40\text{ nm}\times 40\text{ nm}$ .

sensor operated in STM mode at low temperatures. Raw data of an atomically resolved STM image on a Ag(111) single crystal surface at 4 K are presented [Fig. 7(a)]. Single silver atoms on Ag(111) and the surface state waves are shown in Fig. 7(b). These STM measurements confirm the high stability of the microscope as well as the high stiffness and stability of the double tuning fork sensor. An example of operation in AFM mode is given in Figs. 8(a) and 8(b). Both images were taken at the same position on a thin alumina film grown on a NiAl(110) surface. Figure 8(a) shows an image of a monatomic step obtained in STM mode. The same step was then imaged afterward in dynamic AFM mode [Fig. 8(b)]. The image was obtained for a constant frequency shift of  $\Delta f=-50.0$  Hz and amplitude  $A=0.1$  nm. The resolution in the  $z$  direction is better than  $1\text{ \AA}$ , which has been calculated from the imaged step height of approximately  $2\text{ \AA}$ . We are currently optimizing the setup and trying to use different tuning forks as well as optimized tip preparation for a high aspect ratio tip in order to achieve atomic resolution in AFM mode on thin alumina films grown on NiAl(110).<sup>34,35</sup>

#### ACKNOWLEDGMENTS

The authors thank W. Matthees for his contribution of the simulations of the vibrational eigen-modes, and L. Cramer, U. D. Schwarz, T. P. Pearl, and F. J. Giessibl for very fruitful discussions on the use of tuning forks as a force sensor. Furthermore, the authors would like to acknowledge G. Thielsch for technical support and G. Heyne and P. Ziel-ske for advice on electronics. Financial support from the German Science Foundation under SFB 290 TPA9 (M.H.) and the Studienstiftung des deutschen Volkes (M.K.) is gratefully acknowledged.

<sup>1</sup>H. J. Hug, B. Stiefel, P. J. A. van Schendel, A. Moser, S. Martin, and H.-J. Güntherodt, Rev. Sci. Instrum. **70**, 3625 (1999).

<sup>2</sup>F. J. Giessibl, C. Gerber, and G. Binnig, J. Vac. Sci. Technol. B **9**, 984 (1991).

<sup>3</sup>T. Albrecht, P. Grütter, D. Rugar, and D. Smith, Ultramicroscopy **42-44**, 1638 (1992).

<sup>4</sup>W. Allers, A. Schwarz, U. D. Schwarz, and R. Wiesendanger, Rev. Sci. Instrum. **69**, 221 (1998).

<sup>5</sup>Q. Dai, R. Vollmer, R. W. Carpick, D. F. Ogletree, and M. Salmeron, Rev. Sci. Instrum. **66**, 5266 (1995).

<sup>6</sup>K. S. Kitamura and M. Iwatsuki, Jpn. J. Appl. Phys., Part 2 **34**, L145 (1995).

- <sup>7</sup>F. J. Giessibl, *Jpn. J. Appl. Phys., Part 1* **3**, 3726 (1994).
- <sup>8</sup>C. W. Yuan, E. Batalla, M. Zacher, A. L. Lozanne, M. D. Kirk, and M. Tortonese, *Appl. Phys. Lett.* **65**, 1308 (1994).
- <sup>9</sup>J. Rychen, T. Ihn, P. Studerus, A. Hermann, and K. Ensslin, *Rev. Sci. Instrum.* **70**, 2765 (1999).
- <sup>10</sup>F. J. Giessibl, *Appl. Phys. Lett.* **73**, 3956 (1998).
- <sup>11</sup>S. Hembacher, F. J. Giessibl, J. Mannhart, and C. F. Quate, *Proc. Natl. Acad. Sci. U.S.A.* **100**, 12539 (2003) (published after submission).
- <sup>12</sup>T. R. Albrecht, P. Grütter, D. Horne, and D. Rugar, *J. Appl. Phys.* **69**, 668 (1991).
- <sup>13</sup>R. Garcia and R. Perez, *Surf. Sci. Rep.* **47**, 197 (2002).
- <sup>14</sup>F. J. Giessibl, *Appl. Phys. Lett.* **76**, 1470 (2000).
- <sup>15</sup>P. Günther, U. Fischer, and K. Dransfeld, *Appl. Phys. B: Photophys. Laser Chem.* **B48**, 89 (1989).
- <sup>16</sup>K. Karrai and R. Grober, *Appl. Phys. Lett.* **66**, 1842 (1995).
- <sup>17</sup>H. Edwards, L. Taylor, W. Duncan, and A. Melmed, *J. Appl. Phys.* **82**, 980 (1997).
- <sup>18</sup>M. Todorovic and S. Schultz, *J. Appl. Phys.* **83**, 6229 (1998).
- <sup>19</sup>p. c. W. Matthees, Federal Institute for Materials Research and Testing (BAM), Unter den Eichen 87, D-12205 Berlin, Germany.
- <sup>20</sup>O. Pfeiffer, R. Bennewitz, A. Baratoff, E. Meyer, and P. Grütter, *Phys. Rev. B* **65**, 164103 (2002).
- <sup>21</sup>Quartz 304-447, RS Components GmbH, Hessenring 13b, D-64546 Mörfelden-Walldorf, Germany.
- <sup>22</sup>I. Szabó, *Einführung in die Technische Mechanik*, 6th ed. (Springer, Berlin, 1963).
- <sup>23</sup>Torr Seal Resin Sealant, Varian Vacuum Technologies, 121 Hartwell Avenue, Lexington, MA 02421.
- <sup>24</sup>M. Kulawik, M. Nowicki, G. Thielsch, L. Cramer, H.-P. Rust, H.-J. Freund, T. P. Pearl, and P. S. Weiss, *Rev. Sci. Instrum.* **74**, 1027 (2003).
- <sup>25</sup>Audio Transformer 210-6380, RS Components GmbH, Hessenring 13b, D-64546 Mörfelden-Walldorf, Germany
- <sup>26</sup>3N163, Vishay Electronic GmbH, Geheimrat-Rosenthal-Str. 100, D-95100 Selb, Germany.
- <sup>27</sup>D. Sarid, *Scanning Force Microscopy*, revised ed. (Oxford University Press, New York, 1994).
- <sup>28</sup>Nanosurf AG, Grammetstrasse 14, Ch-4410 Liestal, Swiss.
- <sup>29</sup>P. S. Weiss and D. M. Eigler, in *Nanosources and Manipulations of Atoms Under High Fields and Temperatures: Applications*, NATO ASI Ser. E Vol. 235, edited by V. T. Binh, N. Garcia, and K. Dransfeld (Plenum, New York, 1993).
- <sup>30</sup>H.-P. Rust, J. Buisset, E. K. Schweizer, and L. Cramer, *Rev. Sci. Instrum.* **68**, 129 (1997).
- <sup>31</sup>H.-P. Rust, M. Doering, J. I. Pascual, T. P. Pearl, and P. S. Weiss, *Rev. Sci. Instrum.* **72**, 4393 (2001).
- <sup>32</sup>Halcyonics GmbH, Tuchmacherweg 12, D-37079 Göttingen, Germany.
- <sup>33</sup>Nanotec Electronica, Parque Científico de Madrid, Pabellon C, Campus UAM, Cantoblanco, E-28049 Madrid, Spain.
- <sup>34</sup>G. Ceballos, Z. Song, J. I. Pascual, H.-P. Rust, H. Conrad, M. Bäumer, and H.-J. Freund, *Chem. Phys. Lett.* **359**, 41 (2002).
- <sup>35</sup>M. Kulawik, N. Nilius, H.-P. Rust, and H.-J. Freund, *Phys. Rev. Lett.* **91**, 256101 (2003).